

A Fibulin-1 Homolog Interacts with an ADAM Protease that Controls Cell Migration in *C. elegans*

Yukihiko Kubota, Rie Kuroki, and Kiyoji Nishiwaki*
RIKEN Center for Developmental Biology
Chuo-ku
Kobe 650-0047
Japan

Summary

ADAM (a disintegrin and metalloprotease) family proteins play important roles in animal development and pathogenesis [1]. In *C. elegans*, a secreted ADAM protein, MIG-17, acts from outside the gonad to control the migration of gonadal distal tip cells (DTCs) that promote gonad morphogenesis [2]. Here, we report that dominant mutations in the *fbl-1* gene encoding fibulin-1 spliced isoforms, which are calcium binding extracellular matrix proteins, bypass the requirement for MIG-17 activity in directing DTC migration. Specific amino acid substitutions in the third EGF-like motif of one of the two isoforms, FBL-1C, which corresponds to mammalian fibulin-1C, suppress *mig-17* mutations. FBL-1C is synthesized in the gut cells and localizes strongly to the gonadal basement membrane in a MIG-17-dependent manner. Localization of mutant FBL-1C is weaker than that of the wild-type protein and is insensitive to MIG-17 activity, suggesting that it gains a novel function that compensates for its reduced molecular density. We propose that proteolysis by MIG-17 recruits FBL-1C to the gonadal basement membrane, where it is required for the guidance of DTCs, and that mutant FBL-1C acts in a manner that mimics the downstream events of MIG-17-mediated proteolysis.

Results and Discussion

Suppressors of Cell Migration Defects Caused by Loss of MIG-17 Activity

Several members of the ADAM family of proteins function in cell migration through cell surface binding and proteolytic activity [1]. In *C. elegans*, two secreted ADAM proteins, MIG-17 and GON-1 [3], are required for the control of DTC migration during development of the hermaphrodite gonad. The DTCs migrate over the body wall basement membrane in a U-shaped pattern to direct morphogenesis of the gonad arms [4, 5] (Figures 1A and 1B). GON-1 is required for the DTC migration itself, whereas MIG-17 functions to control the route of migration [2, 3]. To understand the molecular mechanisms required for MIG-17-dependent control of cell migration, we investigated suppressor mutations that can suppress the defects of DTC migration in *mig-17* mutants. We found that these suppressor mutations were alleles of *fbl-1*, a gene encoding fibulin-1 homologs.

Mutations in the *fbl-1* gene were recovered from a genetic screen designed to identify mutations that sup-

press DTC migration defects in *mig-17(k174)*, a putative null allele that has a termination codon in the prodomain (Figure 2A). The DTCs in *mig-17* mutants migrate over the ventral body wall muscle in a normal manner, but the migration path deviates from the normal route after the first turn; it often meanders on the lateral hypodermis or dorsal muscle (Figure 1C; Figure 2A). The two *fbl-1* mutations, *k201* and *k206*, strongly suppressed all of these phenotypes associated with *mig-17(k174)* mutants (Figures 1D and 1E; Figure 2A). They also suppressed *mig-17* missense mutations *k135* and *k169*, indicating that the suppression is not specific for *mig-17(k174)* (Figure 2A). Because *fbl-1* mutations suppressed *mig-17* mutants moderately in heterozygotes (Figure 2B), we asked whether they constitute loss-of-function or gain-of-function mutations. Using a deficiency *eDf19* deleting the *fbl-1* locus, we found that *eDf19/+* did not suppress *mig-17(k174)*, suggesting that the suppressors are gain-of-function alleles of the *fbl-1* locus (Figure 2A).

Mutations in Fibulin-1 Homologs Suppress *mig-17* Defects

The *fbl-1* gene was molecularly cloned and found to be equivalent to the predicted gene *F56H11.1*, which encodes proteins highly homologous to the human fibulin-1 isoforms. Mammalian fibulins are calcium binding proteins that associate with the basement membrane, elastic extracellular matrix fibers, or blood plasma [6]. In cultured cells, fibulins affect cell migration or cell-substratum attachment [7, 8, 9]. *fbl-1* encodes at least two splicing variants; FBL-1C and FBL-1D correspond to human fibulin-1C and fibulin-1D, respectively [10] (Figure 3A). FBL-1C and FBL-1D differ only in their C-terminal domains. Each protein contains an N-terminal signal peptide followed by three anaphylatoxin-like repeats and nine epidermal growth factor (EGF)-like repeats, eight of which are related to the Ca²⁺ binding EGF-like motif. Interestingly, suppressor *fbl-1* mutations were found to occur at specific amino acid residues in the third EGF-like repeat, these residues being conserved among *C. elegans*, human [11], chicken [10], and zebrafish [12]. Glycine-249 was changed to glutamate in mutants *k201* and *tk51*, and histidine-251 was changed to tyrosine in *k206*. These amino acids likely constitute the loop region in the calcium binding EGF-like module deduced from the structure of that of human fibrillin [13] (Figure 3A).

We investigated the functions of wild-type and mutant FBL-1 in DTC migration with gene dosage analyses (Figure 2B). When we introduced extrachromosomal arrays containing multicopy *fbl-1(k201)* or *fbl-1(k206)* mutant genes into *mig-17* mutants, they partially suppressed the migration defects as the *fbl-1* heterozygotes do. Interestingly, the introduction of the wild-type *fbl-1* array into *fbl-1(k201); mig-17(k174)* animals abolished the suppression effect of the endogenous gain-of-function *fbl-1(k201)* allele. The wild-type *fbl-1* array enhanced

*Correspondence: nishiwak@cdb.riken.go.jp

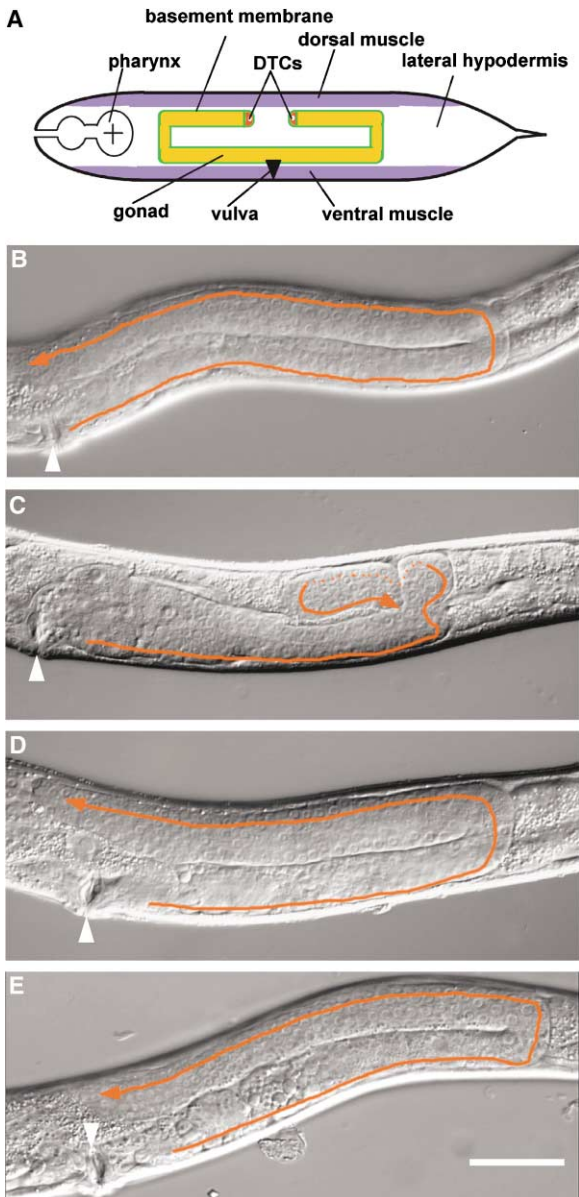


Figure 1. Wild-type and Mutant Gonad Morphology

(A) Gonad morphology in wild-type hermaphrodites. The gonad primordium lies at the center of the body over the ventral body wall muscle during the first larval (L1) stage. The two DTCs formed at the tips of the gonad migrate both anteriorly and posteriorly during the L2 and early L3 stages. The DTCs turn dorsally during mid-L3 and migrate across the lateral hypodermis. They turn again over the dorsal muscle around the time of the L3 molt and subsequently migrate toward each other along the dorsal muscle, thereby generating symmetrical U-shaped gonad arms.

(B–E) Nomarski images of the posterior gonad arms of wild-type (B), *mig-17(k174)* (C), *fbl-1(k201); mig-17(k174)* (D), and *fbl-1(k206); mig-17(k174)* (E). The migratory routes of DTCs are depicted by red lines and arrowheads. Arrowheads point to the vulva. The scale bar represents 50 μm .

the migration defects of *mig-17(k174)* single mutants. However, the *fbl-1(k201)* array had no effect on *fbl-1(k201); mig-17(k174)* animals. These observations sug-

gest that the gain-of-function and wild-type FBL-1 proteins have opposite effects on DTC migration and that they exhibit dose-dependent competition in the absence of MIG-17; that is, wild-type FBL-1 interferes with directed DTC migration, whereas mutant FBL-1 allows it.

The *fbl-1* Deletion Mutant Is Defective in Gonad Development

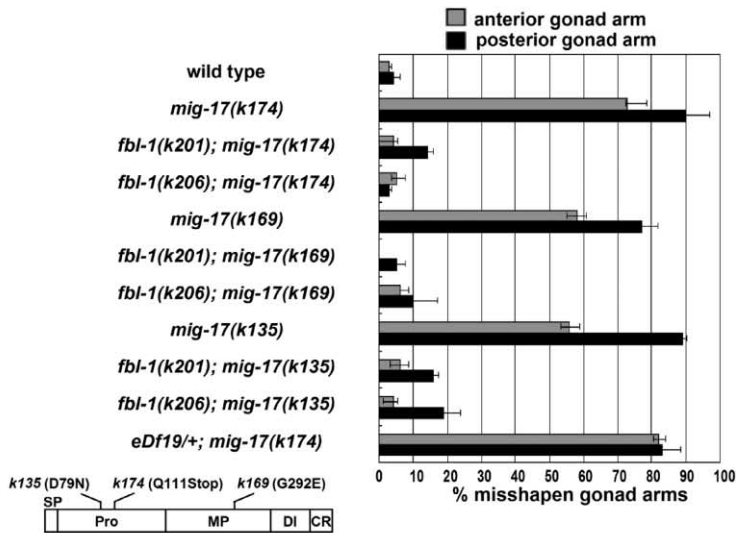
To further examine the function of *fbl-1*, we isolated deletion mutants with the trimethylpsoralen and UV irradiation method [14, 15] (see Experimental Procedures). The *fbl-1(tk45)* mutation is a 358 bp deletion from the last nucleotide of the fourth exon into the fourth intron; it is predicted to introduce a stop codon shortly after the coding region of the first EGF-like motif (Figure 3A). The *fbl-1(tk45)* hermaphrodites had severe defects in gonad morphology and were sterile. Although *tk45* animals were somewhat dumpy, they showed essentially normal sinusoidal movement. In the *tk45* mutants, the proximal arms of the gonads gradually distended after the first turn of the DTCs and became very thick late in the L4 stage (Figures 4A–4D). The anterior DTCs often failed to make the first turn, and the posterior DTCs migrated erratically after the first turn and ceased migration halfway along the dorsal muscle after the second turn (Figures 4C and 4D). The germline cells broke out of the gonad and spread into the body cavity in older adults (Figures 4E and 4F). These phenotypes were fully rescued by introducing wild-type *fbl-1* genomic DNA as a transgenic array. Also, the phenotypes of *tk45/eDf19* animals were similar to those of *tk45* homozygotes (data not shown), suggesting that *tk45* could be a null allele. Double mutants of *mig-17(k174)* and *fbl-1(tk45)* had DTC phenotypes indistinguishable from those of *tk45* single mutants, indicating that *tk45* does not suppress *mig-17* and vice versa. Thus, mutant FBL-1 proteins must be expressed for suppression of *mig-17* to occur.

The germline leakage phenotype has been reported for mutations in laminin subunit genes and is suggested to be a consequence of basement membrane defects [16]. This phenotype is similar to the disruption of blood vessels in fibulin-1-deficient mice [17]. It is likely that depletion of the FBL-1 protein affects the flexibility or strength of the gonadal basement membrane so that it cannot support the extensive proliferation of the germline during the middle to late adult stages. Therefore, FBL-1 proteins have an essential function in maintaining the integrity of the gonadal tube during and after completion of DTC migration.

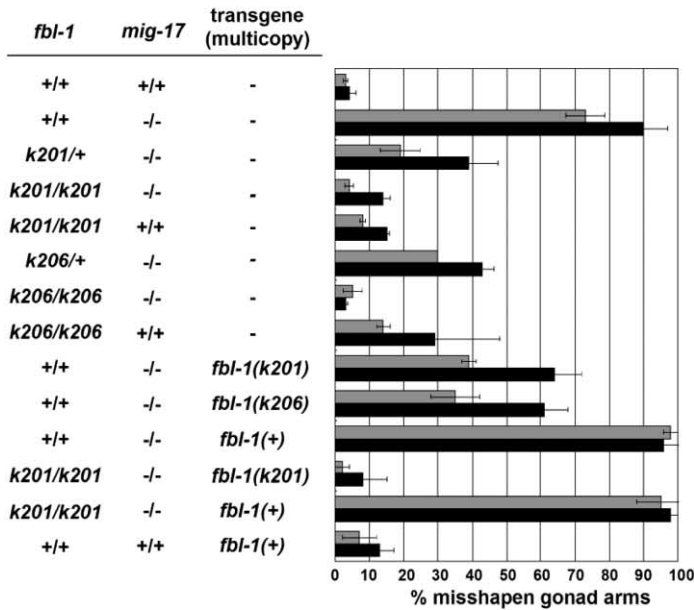
The FBL-1C Protein Localizes to the Gonadal Basement Membrane

We next examined the pattern of *fbl-1* expression. We introduced a fusion gene containing the *fbl-1* promoter and GFP attached to a nuclear localization signal (*fbl-1p::NLS-GFP*) into wild-type hermaphrodites. GFP was strongly expressed at the anterior and posterior ends of intestinal cells as well as in some of the body wall muscle cells in the head, tail, and dorsal side (Figures 5A and 5B). These expression patterns were especially evident in late embryos and early larvae. The expression

A



B



C

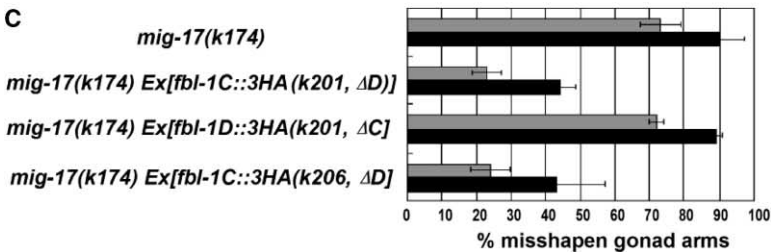


Figure 2. Characterization of Suppressors

(A–C) Percentage of misshapen gonad arms (DTC migration defects) in the anterior (gray) or posterior (black) gonads.

(A) *fbl-1* mutations suppress multiple alleles of *mig-17*. Mutation sites of the relevant *mig-17* alleles are indicated. The following abbreviations were used: SP, signal peptide; Pro, prodomain; MP, metalloprotease domain; DI, disintegrin-like domain; and CR, cysteine-rich domain. n = 60 or 120.

(B) Dosage effects of wild-type and gain-of-function-type *fbl-1* genes on suppression. n = 60 or 120. Note that the DTC migration abnormality was somewhat more pronounced when *fbl-1(k206)* was placed in the wild-type background compared with the *mig-17* mutant background, suggesting that the loss of MIG-17 activity also suppresses DTC migration defects induced by the *k206* mutation.

(C) Isoform-specific suppression of *mig-17(k174)*. See Figure 3B for transgene constructs. n = 120. All error bars represent the mean ± the standard deviation.

in the intestinal cells gradually expanded to the central region during the later larval stages.

To determine the distribution of FBL-1 proteins, we used the yellow fluorescent protein variant Venus [18]. We constructed fusion genes containing Venus coding regions inserted immediately after the C-terminal exons of FBL-1C (*fbl-1C::Venus*) or FBL-1D (*fbl-1D::Venus*) (Figure 3B). Western blot analysis with an anti-GFP anti-

body detected a 125 kDa protein for FBL-1C and 127 and 98 kDa proteins for FBL-1D (Figure 5J). FBL-1C-Venus was expressed at the anterior and posterior ends of intestinal cells and localized to the gonadal and pharyngeal basement membranes (Figure 5C; see also Figure S1 in the Supplemental Data available with this article online). FBL-1D-Venus was strongly expressed in some of the body wall muscle cells in the head and tail

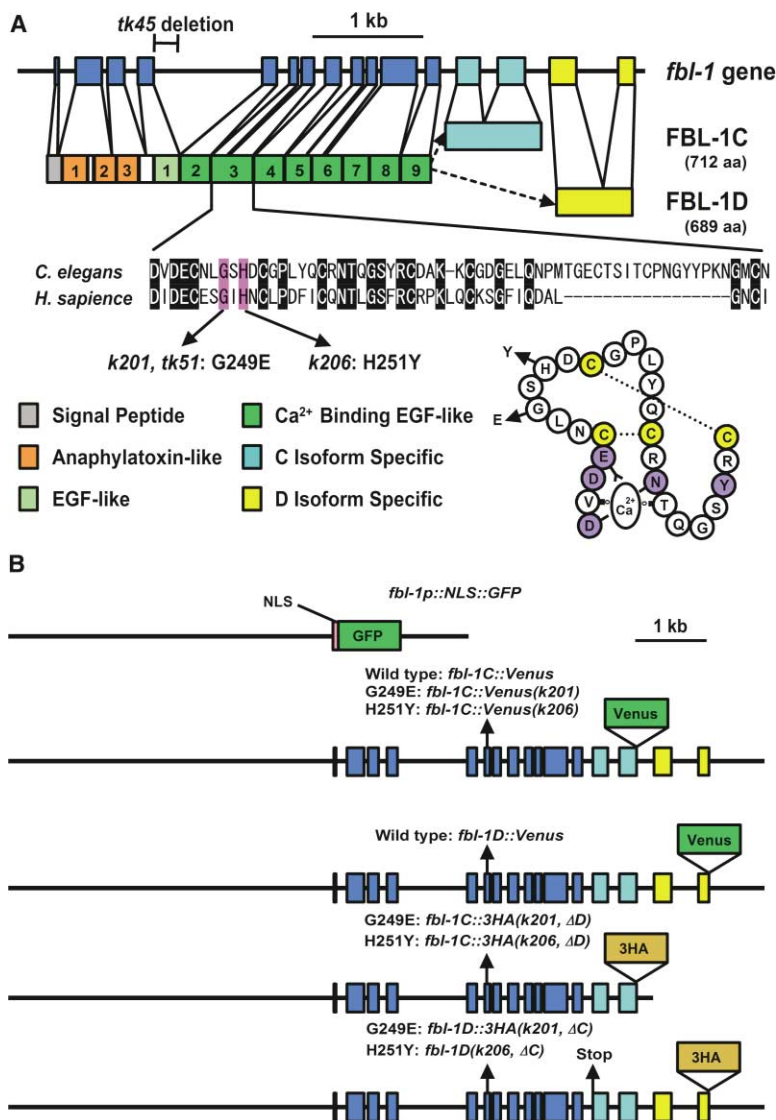


Figure 3. Structures of the *fbl-1* Genes and Constructs Used in Transgenic Analyses

(A) Structures of the wild-type and mutant *fbl-1* genes and gene products. The cDNA and amino acid sequences for FBL-1D are from [10], and those for FBL-1C are from the sequence of cDNA yk1086a09. Exons are shown by colored boxes. Alternatively spliced exons corresponding to the FBL-1C-specific C-terminal domain are shown in light blue, and those for FBL-1D are in yellow. The deleted region in the *tk45* mutation is indicated. The following protein structures are indicated: signal peptide (gray), anaphylatoxin-like module (orange), EGF-like module (light green), Ca²⁺ binding EGF-like module (dark green), C-isoform-specific domain (light blue), and D-isoform-specific domain (yellow). The anaphylatoxin- and EGF-like modules are numbered. The third EGF-like module's amino acid sequence is shown aligned with the corresponding sequence of human fibulin-1. Amino acid substitutions in *k201* or *tk51* G249E (GGA to GAA) and *k206* H251Y (CAT to TAT) are indicated. The folded structure of the third EGF-like module deduced from that of human fibrillin [13] is shown. The Ca²⁺ binding consensus residues and cysteine residues are shown in purple and yellow, respectively. The disulphide bonds are indicated with dashed lines. The amino acid substitutions in the *fbl-1* mutants are indicated.

(B) Constructs used in transgenic experiments. The insertion sites of the GFP-, Venus-, or 3HA-encoding fragments are indicated. The *fbl-1D* (*k206*, Δ C) construct does not have 3HA. The transcriptional terminators are those of the endogenous genomic regions, except for *fbl-1p::NLS::GFP*, in which the *unc-54* terminator was used.

(data not shown). However, the FBL-1D-Venus was not detected in basement membranes. Both *fbl-1C::Venus* and *fbl-1D::Venus* constructs rescued *fbl-1(tk45)* mutants, suggesting that Venus fusion proteins are functional.

FBL-1C, but Not FBL-1D, Is Required for the Suppression of *mig-17* Defects

We tested whether isoform FBL-1C or FBL-1D is essential for the suppression of *mig-17* defects. We constructed *fbl-1(k201)* or *fbl-1(k206)* mutant genes in which the D-isoform-specific C-terminal domain was deleted (see *fbl-1C::3HA(k201, Δ D)* and *fbl-1C::3HA(k206, Δ D)* in Figure 3B). Transgenic arrays containing either of these genes suppressed the DTC migration defects of *mig-17(k174)* (Figure 2C). We also constructed mutant genes containing a termination codon early in the coding region of the C-isoform-specific C-terminal domain (see *fbl-1D::3HA(k201, Δ C)* and *fbl-1D(k206, Δ C)* in Figure 3B). They failed to suppress *mig-17* phenotypes when introduced as transgenic arrays (Figure 2C; data not

shown for *fbl-1D(k206, Δ C)*). We confirmed the expression of the tagged mutant proteins by Western blotting (Figure S2). These results indicate that the C isoform, but not the D isoform, is essential for the suppression of *mig-17* phenotypes.

Because FBL-1C-Venus localized to the gonadal basement membrane, we examined whether this localization is affected by *mig-17* mutations. We found that substantially less FBL-1C-Venus localized to the gonad surface when it was expressed in the *mig-17* mutant background (Figure S3A). Because ectopic expression of membrane-anchored MIG-17 under the control of the DTC-specific *lag-2* promoter rescues the DTC migration defects of *mig-17* mutants (K. Nishiwaki, unpublished data), we examined the localization of FBL-1C in such transgenic animals. FBL-1C-Venus specifically accumulated on the surface of DTCs in rescued animals (Figure S3B). Therefore, the MIG-17 activity in the microenvironment of the gonad surface is required for efficient localization of FBL-1C to the gonad.

We then constructed mutant versions of the *fbl-*

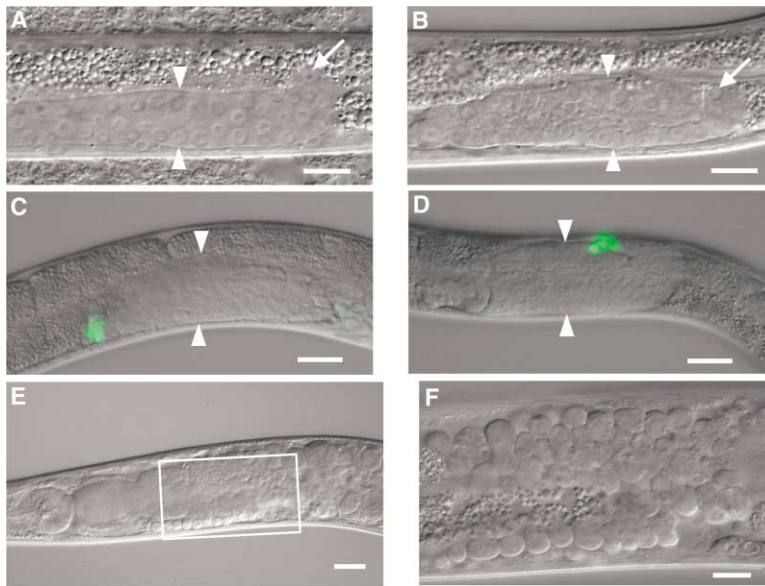


Figure 4. Gonadal Defects in *fbl-1(tk45)* Deletion Mutants

Photos are oriented anterior to the left and dorsal to the top.

(A and B) Late L3 hermaphrodite. The gonadal tubes in *fbl-1(tk45)* (B) begin to thicken when compared to those in *tk45/+* (A) around the first turn of the DTCs (arrowheads). The arrow points to the DTC.

(C and D) *fbl-1(tk45)* late L4 hermaphrodites with an integrated *lag-2p::GFP* array, *qls51*. Proximal gonad arms are very thick (arrowheads). The anterior DTC failed to make the first turn (C), and the posterior DTC ceased migrating when it was halfway along the dorsal muscle after the second turn (D). The fluorescence images of DTCs expressing GFP were overlaid with the Nomarski images.

(E) *fbl-1(tk45)* 2–3-day-old adult hermaphrodites. The germline cells broke out of the gonad and spread into the body cavity.

(F) Magnified image of the boxed area in (E). The focal plane is slightly higher than in (E). The scale bars represent 10 μm in (A), (B), and (F) and 20 μm in (C)–(E).

1C::Venus fusion genes, *fbl-1C::Venus(k201)* and *fbl-1C::Venus(k206)*, and examined the protein localization in the *fbl-1(tk45)* mutant background. Both the wild-type and mutant *fbl-1::Venus* fusion constructs rescued the sterility of *tk45*, and the gonadal accumulation of the expressed proteins was seen more clearly in the *tk45* than in the wild-type background (compare Figures 5C and 5D). The gonadal localization of wild-type FBL-1C-Venus was stronger compared to the FBL-1C-Venus (*k201*) and FBL-1C-Venus(*k206*) mutant proteins, whose patterns of accumulation were weak irrespective of the *mig-17* background (Figures 5D–5F; data not shown for *k201*). We found that the gonadal localization of FBL-1C-Venus is stronger than that of FBL-1C-Venus(*k206*) in the dissected gonads (Figures 5G–5I). Furthermore, the level of expression of FBL-1C-Venus(*k206*) was comparable to that of FBL-1C-Venus (Figure 5K), suggesting that the stabilities of wild-type and mutant FBL-1C proteins are similar. These observations suggest that the mutant FBL-1C proteins have a weaker affinity for the gonadal basement membrane than the wild-type protein and that they are insensitive to the MIG-17 activity.

Possible Function of FBL-1 Proteins in MIG-17-Dependent Control of Cell Migration

Several models can be considered for the mechanisms of suppression. Because MIG-17 is normally required for proper guidance of DTCs, MIG-17-mediated proteolysis could create an appropriate extracellular environment for the proper function of guidance molecules, such as UNC-6 (netrin), or for their receptors, such as UNC-5 or UNC-40 [19]. The FBL-1 proteins might be direct targets of MIG-17, and MIG-17-mediated proteolytic cleavage of FBL-1 may be required for such basement membrane remodeling. However, the Western blot analyses of tagged FBL-1 proteins in wild-type or mutant *mig-17* background do not seem to indicate this possibility (Y. Kubota, unpublished data). Given that MIG-17 function is required for proper localization of FBL-1C to the

gonadal basement membrane, MIG-17 seems to act on unknown substrates to promote remodeling of the gonadal basement membrane, which enhances its affinity for FBL-1C. Although it is expected that the mutant FBL-1C proteins would localize strongly in the absence of MIG-17 function, this is not the case. Rather, they seemed to become insensitive to the MIG-17 activity. These observations suggest that specific amino acid substitutions found in the third EGF-like motif endow FBL-1C with a novel function that compensates for the loss of MIG-17 activity in the basement membrane. The calcium binding EGF-like modules are important for protein-protein interactions in the extracellular matrix. Mammalian fibulin-1 binds nidogen-1, laminin-1, aggrecan, and versican in a calcium-dependent manner [20, 21, 22]. In particular, the binding of fibulin-1 to nidogen-1, aggrecan, and versican is mediated by the fibulin-1 domain containing the calcium binding EGF-like modules [21]. We speculate that the amino acid changes in the third EGF-like motif of suppressor FBL-1 proteins may affect their binding specificity or avidity for nidogen, laminin, or proteoglycans, thereby mimicking the MIG-17-dependent remodeling of the gonadal basement membrane in *C. elegans*. It is intriguing that some of the mammalian ADAM with thrombospondin motifs (ADAMTS) proteins, which are structurally similar to MIG-17, catalyze the hydrolysis of proteoglycans [23, 24]. Although the functions of FBL-1/fibulin-1 remain elusive, our findings, together with the finding that *fbl-1* suppresses the mutations in *gon-1*, another gene for an ADAM protease ([25], this issue of *Current Biology*), strongly suggest that, in addition to its function in maintaining the structural integrity of the extracellular matrix, it has critical roles in controlling directed cell migration via interactions with secreted ADAM proteases.

Experimental Procedures

Genetic Analysis

mig-17 mutants have ventral white patch phenotypes under a dissecting microscope [26]. Suppressor mutants were isolated by the

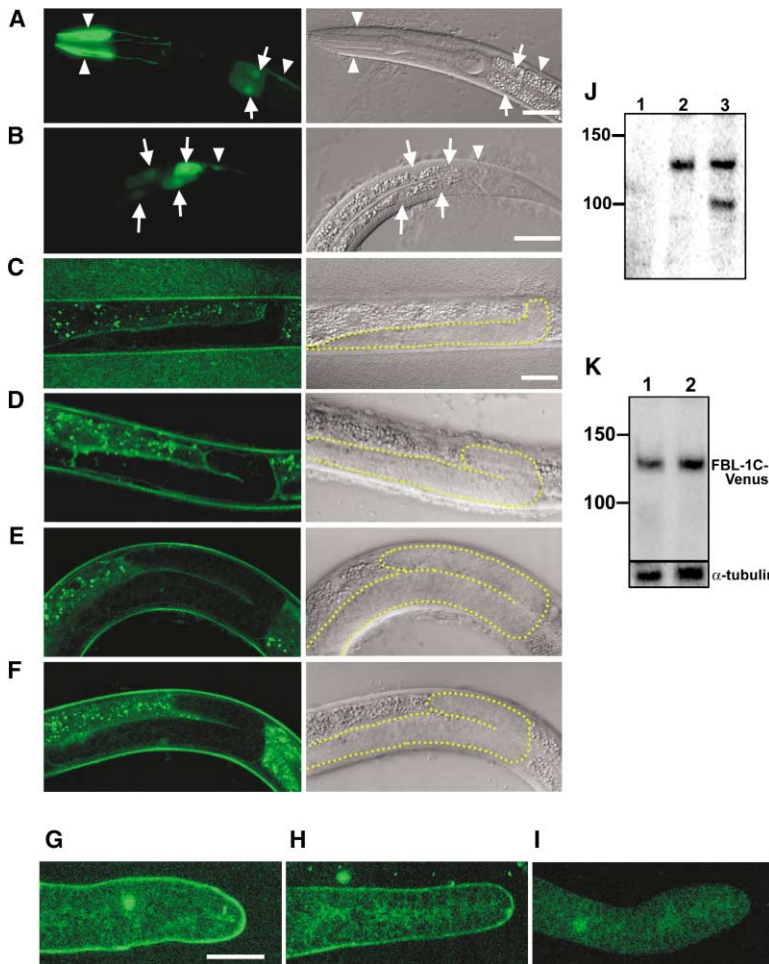


Figure 5. Expression Patterns of FBL-1 Proteins

Photos are oriented anterior to the left and dorsal to the top.

(A and B) Fluorescence (left) and Nomarski (right) images of head (A) and tail (B) regions of wild-type L2 hermaphrodites expressing *fbl-1p::NLS::GFP*. GFP was expressed in the intestine (arrows) and the body wall muscles (arrowhead).

(C) Confocal (left) and Nomarski (right) images of a late L3 (C) wild-type hermaphrodite expressing *fbl-1C::Venus*. FBL-1C-Venus localized to the surface of the gonads. The boundary of the gonad is depicted by a dotted line in the Nomarski image (also for [D]–[F]). Punctate fluorescence outside the gonads is of the FBL-1C-Venus in the Golgi apparatus of the gut cells or autofluorescence of the gut granules. The expression of *fbl-1C::Venus* is especially strong in gut cells posterior to the gonad. The same is true in (D)–(F).

(D and E) Confocal (left) and Nomarski (right) images of *fbl-1(tk45)* L4 hermaphrodites expressing *fbl-1C::Venus* (D) and *fbl-1C::Venus(k206)* (E). The accumulation of FBL-1C-Venus is stronger than that of FBL-1C-Venus(k206).

(F) Confocal (left) and Nomarski (right) images of *fbl-1(tk45); mig-17(k174)* L4 hermaphrodites expressing *fbl-1C::Venus(k206)* (F). FBL-1C-Venus(k206) localizes to the surface of the gonads as in (E).

(G and H) Confocal images of dissected gonads of *fbl-1(tk45)* hermaphrodites expressing *fbl-1C::Venus* (G) and *fbl-1C::Venus(k206)* (H).

(I) Confocal image of wild-type hermaphrodite with no transgene. The scale bars represent 20 μ m. The scale bar in (C) is also applicable to (D)–(F), and the scale bar in (G) is also applicable to (H) and (I).

(J and K) Western analysis of Venus fusion proteins with anti-GFP antibody.

(J) Extracts from wild-type hermaphrodites with no transgene (lane 1), *fbl-1C::Venus* (lane 2), or *fbl-1D::Venus* (lane 3) were immunoblotted. (K) Extracts from *fbl-1(tk45)* hermaphrodites expressing *fbl-1C::Venus* (lane 1) and *fbl-1C::Venus(k206)* (lane 2) were immunoblotted. α -tubulin was used as a loading control.

visual screening of F1 or F2 animals in which the normal body-color pattern was restored from *mig-17(k174)* hermaphrodites treated with ethylmethane sulfonate [27]. *fbl-1* mutations *k201*, *k206*, and *tk51* were semidominant and mapped to the central region of the linkage group IV. *fbl-1(k201)* was further mapped genetically to a 130 kb genomic region between cosmid clones C33A12 and W09C2 by SNP mapping. A search for DNA sequence alterations in this region identified mutations in the predicted gene *F56H11.1*. *F56H11.1* was also altered in two other *fbl-1* mutants, *k206* and *tk51*, isolated independently. Since the *fbl-1* mutations seemed to be semidominant gain-of-function mutations, we reasoned that the mutant *fbl-1* genes would be able to suppress *mig-17* defects when they were introduced as transgenes. As expected, extrachromosomal arrays containing multiple copies of the mutant *F56H11.1* genes from either the *fbl-1(k201)* or *fbl-1(k206)* genomic DNAs suppressed the DTC migration defects of *mig-17*. The JK2868 strain, containing an integrated *lag-2p::GFP* plasmid, was used to construct animals with GFP-labeled DTCs. A deletion mutant, *fbl-1(tk45)*, was isolated by the trimethylpsoralen and UV irradiation method [14, 15]. The production of a knockout mutant bank and screening of deletion mutants were done according to the protocol by Hitoshi Inada and Ikuo Mori (<http://bunshi3.bio.nagoya-u.ac.jp/bunshi0/PagesJ/TMP-UV.html>). Animals were cultured at 20°C in all experiments.

Molecular Methods

The *fbl-1* cDNA yk1086a09 was kindly provided by Yuji Kohara. The sequencing of this cDNA revealed that it corresponds to the mRNA

for the FBL-1C isoform. The 4503 bp *fbl-1* promoter region corresponding to nucleotide positions 11171–15683 on cosmid clone F56H11 was amplified by PCR and inserted into the SphI and BamHI sites of pKOGzero to make the *fbl-1p::NLS-GFP* plasmid [28]. A 12876 bp KpnI-XhoI fragment of the *fbl-1* gene from a fosmid clone, H18K20, was subcloned into the pBSIIKS(–) vector to make plasmid pYK1. The modified *fbl-1* gene constructs used in this work were generated from pYK1. The plasmid carrying the *Venus* gene was kindly provided by Takeshi Ishihara. The *fbl-1C::Venus* and *fbl-1D::Venus* fusion genes were constructed by inserting PCR-amplified *Venus*-encoding fragments into the positions immediately before the termination codons of the *fbl-1C* and *fbl-1D* coding regions, respectively. The *fbl-1C::Venus(k201)* and *fbl-1C::Venus(k206)* genes were constructed by replacing the Apal-Ball fragment of *fbl-1C::Venus* with Apal-Ball PCR-amplified fragments of the mutant genomic DNAs. The *fbl-1(k201)* or *fbl-1(k206)* mutant genes were similarly generated by fragment swapping. *fbl-1(k201, Δ D)* and *fbl-1(k206, Δ D)* were constructed by deleting the fragment downstream of the 14th intron of *fbl-1(k201)* and *fbl-1(k206)*, respectively. The *fbl-1(k201, Δ C)* and *fbl-1(k206, Δ C)* genes were constructed by site-directed mutagenesis (Stratagene, La Jolla, CA), which changed the cysteine codon of the 565th amino acid of FBL-1C into a stop codon (TGT to TGA) in the *fbl-1(k201)* and *fbl-1(k206)* genes, respectively. *fbl-1C::3HA(k201, Δ D)*, *fbl-1C::3HA(k206, Δ D)*, and *fbl-1D::3HA(k201, Δ C)* were generated from these constructs. For Western blot analysis, mixed populations of worms grown at 20°C were collected and sonicated in 50 mM Tris-HCl (pH 8.0), 150 mM NaCl, 10% glycerol, 1% Triton X-100, 5 mM phenylmethylsulfonyl fluoride, 1 μ g/ml leu-

peptin, and 1 $\mu\text{g/ml}$ pepstatin to prepare the lysate. 20 μg of protein was loaded for each sample. Samples were immunoblotted with rabbit anti-GFP IgG (Molecular Probes, Eugene, OR), rat anti-HA IgG 3F10 (Roche Applied Science, Indianapolis, IN), or mouse anti- α -tubulin IgG 12G10 (J. Frankel and M. Nelson) at room temperature for 1 hr and peroxidase-conjugated anti-rabbit IgG, anti-mouse IgG (Amersham Biosciences, Piscataway, NJ), or anti-rat IgG (Jackson ImmunoResearch, West Grove, PA) at room temperature for 1 hr, after which enhanced chemiluminescence (ECL) (Amersham Biosciences) was performed. 12G10 antibodies were provided by the Developmental Studies Hybridoma Bank at the University of Iowa.

Production of Transgenic Animals

Young adult hermaphrodites were used for microinjection, and heritable transgenic lines were obtained from the offspring [29]. For gene dosage analyses, *fbl-1* wild-type or mutant genomic regions were PCR-amplified with primers 5'-CGAGTTCTAGCATCCCTT CACGTCGTCTG-3' and 5'-CGGTGCGAAAATGGATTGGTGAAACG ATAC-3' and were injected into the gonad of wild-type, *mig-17(k174)*, and *fbl-1(k201)*; *mig-17(k174)* mutants at 5 $\mu\text{g/ml}$ with 100 $\mu\text{g/ml}$ marker plasmid carrying *sur-5::GFP* [30] and 50 $\mu\text{g/ml}$ pBR322. The *fbl-1p::NLS-GFP* plasmid was injected into the *unc-119(e2498)* gonad at 30 $\mu\text{g/ml}$ with 10 $\mu\text{g/ml}$ *unc-119⁺* plasmid pDP#MM016B [31] and 110 $\mu\text{g/ml}$ pBSIIKS(-). *fbl-1C::Venus*, *fbl-1D::Venus*, *fbl-1C::Venus(k201)*, and *fbl-1C::Venus(k206)* genes were injected into the *unc-119 (e2498)* gonad at 5 $\mu\text{g/ml}$ with 10 $\mu\text{g/ml}$ pDP#MM016B and 130 $\mu\text{g/ml}$ pBSIIKS(-) or 30 $\mu\text{g/ml}$ marker plasmid *lin-44p::GFP* [32] and 130 $\mu\text{g/ml}$ pBSIIKS(-). The *lag-2p::mig-17::TM::2HA* plasmid was injected into the *unc-119 (e2498)* gonad at 20 $\mu\text{g/ml}$ with 10 $\mu\text{g/ml}$ pDP#MM016B, 5 $\mu\text{g/ml}$ *fbl-1C::Venus*, and 115 $\mu\text{g/ml}$ pBSIIKS(-) to construct the *lag-2p::mig-17::TM::2HA* and *fbl-1C::Venus* coexpressing animal. The resulting extrachromosomal arrays were transferred to *mig-17(k174)*; *unc-119(e2498)*, *fbl-1(tk45)*, or *mig-17(k174) unc-42(e270)*; *fbl-1(tk45)* by mating. The plasmids for *fbl-1C::3HA(k201, ΔD)*, *fbl-1C::3HA (k206, ΔD)*, *fbl-1D::3HA(k201, ΔC)*, or *fbl-1D (k206, ΔC)* were injected into the *mig-17(k174)* gonads at 5 $\mu\text{g/ml}$ with 100 $\mu\text{g/ml}$ marker plasmid *sur-5::GFP* and 50 $\mu\text{g/ml}$ pBSIIKS(-).

Gonad Dissection

Animals were placed in a droplet of egg buffer [33] containing 0.2 mM levamisole on a poly-L-lysine-coated slide glass to prepare dissected gonad preparations and were decapitated with a scalpel to extrude the gonads.

Microscopy

Nomarski and fluorescence microscopy were performed with a Zeiss Axioplan 2 microscope equipped with both optical systems. Analysis of the DTC migration phenotypes was as described previously [26]. Images were captured with a Hamamatsu Photonics Color Chilled 3-CCD Camera C5810 (Hamamatsu, Japan) connected to a Macintosh G3 computer. The FBL-1-Venus localizations were analyzed with a Laser-scanning confocal microscope Radiance 2100 Rainbow (Bio-Rad Laboratories, Hercules, CA).

Supplemental Data

Supplemental Figures for this article are available at <http://www.current-biology.com/cgi/content/full/14/22/2011/DC1/>.

Acknowledgments

We thank T. Ishihara, A. Coulson, A. Fire, Y. Kohara, M. Koga, T. Stiernagle, H. Sawa, and the *Caenorhabditis* Genetics Center for materials, H. Inada and I. Mori for the protocol for the construction and screening of a deletion mutant bank, and N. Uodome, M. Sano, and A. Sugimoto for collaboration in constructing the deletion mutant bank. We also thank J. Kimble and D. Hesselson for communicating unpublished results and K. Matsumoto, J. Takagi, S. Ihara, and D. Sipp for critical reading of the manuscript. This work was supported by a Grant-in-Aid for Scientific Research from the Ministry of Education, Culture, and Science of Japan (K.N.).

Received: July 23, 2004

Revised: September 22, 2004

Accepted: September 23, 2004

Published: November 23, 2004

References

1. Seals, D.F., and Courtneidge, S.A. (2003). The ADAMs family of metalloproteases: Multidomain proteins with multiple functions. *Genes Dev.* 17, 7–30.
2. Nishiwaki, K., Hisamoto, N., and Matsumoto, K. (2000). A metalloprotease disintegrin that controls cell migration in *Caenorhabditis elegans*. *Science* 288, 2205–2208.
3. Brelloch, R., and Kimble, J. (1999). Control of organ shape by a secreted metalloprotease in the nematode *Caenorhabditis elegans*. *Nature* 399, 586–590.
4. Kimble, J.E., and White, J.G. (1981). On the control of germ cell development in *C. elegans*. *Dev. Biol.* 81, 208–219.
5. Hedgecock, E.M., Culotti, J.G., Hall, D.H., and Stern, B.D. (1987). Genetics of cell and axon migrations in *Caenorhabditis elegans*. *Development* 100, 365–382.
6. Timpl, R., Sasaki, T., Kostka, G., and Chu, M.-L. (2003). Fibulins: A versatile family of extracellular matrix proteins. *Nat. Rev. Mol. Cell Biol.* 4, 479–489.
7. Qing, J., Maher, V.M., Tran, H., Argraves, W.S., Dunstan, R.W., and McCormick, J.J. (1997). Suppression of anchorage-independent growth and matrigel invasion and delayed tumor formation by elevated expression of fibulin-1D in human fibrosarcoma-derived cell lines. *Oncogene* 15, 2159–2168.
8. Hayashido, Y., Lucas, A., Rougeot, C., Godyna, S., Argraves, W.S., and Rochefort, H. (1998). Estradiol and fibulin-1 inhibit motility of human ovarian- and breast-cancer cells induced by fibronectin. *Int. J. Cancer* 75, 654–658.
9. Twal, W.O., Czirik, A., Hegedus, B., Knaak, C., Chintalapudi, M.R., Okagawa, H., Sugi, Y., and Argraves, W.S. (2001). Fibulin-1 suppression of fibronectin-regulated cell adhesion and motility. *J. Cell Sci.* 114, 4587–4598.
10. Barth, J.L., Argraves, K.M., Roark, E.F., Little, C.D., and Argraves, W.S. (1998). Identification of chicken and *C. elegans* fibulin-1 homologs and characterization of the *C. elegans* fibulin-1 gene. *Matrix Biol.* 17, 635–646.
11. Argraves, W.S., Tran, H., Burgess, W.H., and Dickerson, K. (1990). Fibulin is an extracellular matrix and plasma glycoprotein with repeated domain structure. *J. Cell Biol.* 111, 3155–3164.
12. Zhang, H.-Y., Lardelli, M., and Ekblom, P. (1997). Sequence of zebrafish fibulin-1 and its expression in developing heart and other embryonic organs. *Dev. Genes Evol.* 207, 340–351.
13. Handford, P.A. (2000). Fibrillin-1, a calcium binding protein of extracellular matrix. *Biochim. Biophys. Acta* 1498, 84–90.
14. Barstead, R.J. (1999). Reverse genetics. In *C. elegans: A Practical Approach*, I.A. Hope, ed. (New York: Oxford University Press), pp. 97–118.
15. Gengyo-Ando, K., and Mitani, S. (2000). Characterization of mutations induced by ethyl methanesulfonate, UV, and trimethylpsoralen in the nematode *Caenorhabditis elegans*. *Biochem. Biophys. Res. Commun.* 269, 64–69.
16. Huang, C.C., Hall, D.H., Hedgecock, E.M., Kao, G., Karantza, V., Vogel, B.E., Hutter, H., Chisholm, A.D., Yurchenco, P.D., and Wadsworth, W.G. (2003). Laminin alpha subunits and their role in *C. elegans* development. *Development* 130, 3343–3358.
17. Kostka, G., Giltay, R., Bloch, W., Addicks, K., Timpl, R., Fassler, R., and Chu, M.L. (2001). Perinatal lethality and endothelial cell abnormalities in several vessel compartments of fibulin-1-deficient mice. *Mol. Cell Biol.* 21, 7025–7034.
18. Nagai, T., Ibata, K., Park, E.S., Kubota, M., Mikoshiba, K., and Miyawaki, A. (2002). A variant of yellow fluorescent protein with fast and efficient maturation for cell-biological applications. *Nat. Biotechnol.* 20, 87–90.
19. Hedgecock, E.M., and Norris, C.R. (1997). Netrins evoke mixed reactions in motile cells. *Trends Genet.* 13, 251–253.
20. Sasaki, T., Kostka, G., Gohring, W., Wiedemann, H., Mann, K., Chu, M.L., and Timpl, R. (1995). Structural characterization of two variants of fibulin-1 that differ in nidogen affinity. *J. Mol. Biol.* 245, 241–250.

21. Aspberg, A., Adam, S., Kostka, G., Timpl, R., and Heinegard, D. (1999). Fibulin-1 is a ligand for the C-type lectin domains of aggrecan and versican. *J. Biol. Chem.* *274*, 20444–20449.
22. Ries, A., Gohring, W., Fox, J.W., Timpl, R., and Sasaki, T. (2001). Recombinant domains of mouse nidogen-1 and their binding to basement membrane proteins and monoclonal antibodies. *Eur. J. Biochem.* *268*, 5119–5128.
23. Matthews, R.T., Gary, S.C., Zerillo, C., Pratta, M., Solomon, K., Amer, E.C., and Hockfield, S. (2000). Brain-enriched hyaluronan binding (BEHAB)/brevican cleavage in a glioma cell line is mediated by a disintegrin and metalloproteinase with thrombospondin motifs (ADAMTS) family member. *J. Biol. Chem.* *275*, 22695–22703.
24. Sandy, J.D., Westling, J., Kenagy, R.D., Iruela-Arispe, M.L., Verscharen, C., Rodriguez-Mazaneque, J.C., Zimmermann, D.R., Lemire, J.M., Fischer, J.W., Wight, T.N., et al. (2001). Versican V1 proteolysis in human aorta in vivo occurs at the Glu441-Ala442 bond, a site that is cleaved by recombinant ADAMTS-1 and ADAMTS-4. *J. Biol. Chem.* *276*, 13372–13378.
25. Hesselson, D., Newman, C., Kim, K.W., and Kimble, J. GON-1 and fibulin have antagonistic roles in control of organ shape. *Curr. Biol.* *14*, this issue, 2005–2010.
26. Nishiwaki, K. (1999). Mutations affecting symmetrical migration of distal tip cells in *Caenorhabditis elegans*. *Genetics* *152*, 985–997.
27. Brenner, S. (1974). The genetics of *Caenorhabditis elegans*. *Genetics* *77*, 71–94.
28. Ohkura, K., Suzuki, N., Ishihara, T., and Katsura, I. (2003). SDF-9, a protein tyrosine phosphatase-like molecule, regulates the L3/dauer developmental decision through hormonal signaling in *C. elegans*. *Development* *130*, 3237–3248.
29. Mello, C.C., Kramer, J.M., Stinchcomb, D., and Ambros, V. (1991). Efficient gene transfer in *C. elegans*: Extrachromosomal maintenance and integration of transforming sequences. *EMBO J.* *10*, 3959–3970.
30. Yochem, J., Gu, T., and Han, M. (1998). A new marker for mosaic analysis in *Caenorhabditis elegans* indicates a fusion between *hyp6* and *hyp7*, two major components of hypodermis. *Genetics* *149*, 1323–1334.
31. Maduro, M., and Pilgrim, D. (1995). Identification and cloning of *unc-119*, a gene expressed in the *Caenorhabditis elegans* nervous system. *Genetics* *141*, 977–988.
32. Murakami, M., Koga, M., and Ohshima, Y. (2001). DAF-7/TGF-beta expression required for the normal larval development in *C. elegans* is controlled by a presumed guanylyl cyclase DAF-11. *Mech. Dev.* *109*, 27–35.
33. Edgar, L.G. (1995). Blastomere culture and analysis. *Methods Cell Biol.* *48*, 303–321.